

Incorporating GSA-SPECT into CT-based dose-volume histograms for advanced hepatocellular carcinoma radiotherapy

Shintaro Shirai, Morio Sato, Yasutaka Noda, Yoshitaka Kumayama, Noritaka Shimizu

Shintaro Shirai, Morio Sato, Yasutaka Noda, Yoshitaka Kumayama, Noritaka Shimizu, Department of Radiology, Wakayama Medical University, Wakayama Shi, Wakayama 641-8510, Japan

Author contributions: Shirai S, Sato M, Noda Y, Kumayama Y and Shimizu N contributed to this paper.

Correspondence to: Morio Sato, MD, Professor, Department of Radiology, Wakayama Medical University, 811-1 Kimiidera, Wakayama Shi, Wakayama 641-8510,

Japan. morisato@mail.wakayama-med.ac.jp

Telephone: +81-73-4410604 Fax: +81-73-4443110

Received: December 26, 2013 Revised: April 15, 2014

Accepted: May 28, 2014

Published online: August 28, 2014

Abstract

In single photon emission computed tomography-based three-dimensional radiotherapy (SPECT-B-3DCRT), images of Tc-99m galactosyl human serum albumin (GSA), which bind to receptors on functional liver cells, are merged with the computed tomography simulation images. Functional liver is defined as the area of normal liver where GSA accumulation exceeds that of hepatocellular carcinoma (HCC). In cirrhotic patients with a gigantic, proton-beam-untreatable HCC of ≥ 14 cm in diameter, the use of SPECT-B-3DCRT in combination with transcatheter arterial chemoembolization achieved a 2-year local tumor control rate of 78.6% and a 2-year survival rate of 33.3%. SPECT-B-3DCRT was applied to HCC to preserve as much functional liver as possible. Sixty-four patients with HCC, including 30 with Child B liver cirrhosis, received SPECT-B-3DCRT and none experienced fatal radiation-induced liver disease (RILD). The Child-Pugh score deteriorated by 1 or 2 in $> 20\%$ of functional liver volume that was irradiated with ≥ 20 Gy. The deterioration in the Child-Pugh score decreased when the radiation plan was designed to irradiate $\leq 20\%$ of the functional liver volume in patients given

doses of ≥ 20 Gy ($_{FLV20Gy}$). Therefore, $_{FLV20Gy} \leq 20\%$ may represent a safety index to prevent RILD during 3DCRT for HCC. To supplement $_{FLV20Gy}$ as a qualitative index, we propose a quantitative indicator, F_{20Gy} , which was calculated as $F_{20Gy} = 100\% \times (\text{the GSA count in the area irradiated with } \geq 20 \text{ Gy})/(\text{the GSA count in the whole liver})$.

© 2014 Baishideng Publishing Group Inc. All rights reserved.

Key words: Functional image-guided radiotherapy; Galactosyl human serum albumin; Dose-volume histogram; Three-dimensional radiotherapy; Hepatocellular carcinoma

Core tip: Three-dimensional conformal radiotherapy, which is designed to preserve functional liver, can be visualized by single photon emission computed tomography with Tc-99m-galactosyl human serum albumin (GSA). This treatment modality has promising therapeutic effects for hepatocellular carcinomas (HCCs) of > 14 cm in diameter that are unmanageable by proton beam therapy. A treatment plan designed to irradiate $\leq 20\%$ of the functional liver volume ($_{FLV20Gy} \leq 20\%$) did not cause radiation-induced liver disease. Therefore, $_{FLV20Gy} \leq 20\%$ may be a useful safety marker for three-dimensional radiotherapy of HCC of various sizes. It is also possible to estimate the effects of radiotherapy on the liver by dividing the GSA count in the region of the liver irradiated with ≥ 20 Gy by the GSA count of the entire liver.

Shirai S, Sato M, Noda Y, Kumayama Y, Shimizu N. Incorporating GSA-SPECT into CT-based dose-volume histograms for advanced hepatocellular carcinoma radiotherapy. *World J Radiol* 2014; 6(8): 598-606 Available from: URL: <http://www.wjgnet.com/1949-8470/full/v6/i8/598.htm> DOI: <http://dx.doi.org/10.4329/wjr.v6.i8.598>

INTRODUCTION

The development of computed tomography (CT) has contributed to radiation treatment (RT) planning by its ability to reveal the precise location of target tissue and at-risk organs in three dimensions, thus enabling dose-volume histograms (DVHs) to be created^[1]. The introduction of DVHs has had significant benefits in terms of better target control and reduced adverse effects. However, even in cases where a DVH was used, RT may cause radiation-induced liver disease (RILD), which is sometimes fatal, in patients with advanced hepatocellular carcinoma (HCC)^[2,3]. In the normal tissue complication probability model, which is used to predict disorders based on the DVH, the volume-adverse effect coefficient is relatively large (0.32-0.40)^[4,5]. Therefore, attempts to reduce the irradiation volume do not always prevent RILD^[2,3]. Furthermore, the proportion of irradiated normal liver relative to the entire normal liver (NL/V_{Gy}) often fails to predict RILD^[2,3,6].

The onset of RILD was commonly attributed to the presence of liver cirrhosis in patients with HCC^[2,3]. For example, Ikai *et al*^[7] reported marked variability in the function of normal liver in patients with liver cirrhosis and in patients with portal vein tumor thrombus (PVTT), which led to the adoption of a surgical therapeutic strategy. Radiation oncologists generally use and rely upon CT-based DVH. Many radiation oncologists may not acknowledge or cope with the possible variations in liver function in normal liver.

Because single photon emission computed tomography (SPECT) with liver scintigraphy reflects the function of normal liver^[7-9], we anticipated that SPECT could be used to evaluate localized liver function. Nanashima *et al*^[8] reported that SPECT images obtained using Tc-99m-galactosyl human serum albumin (GSA) provided a better assessment of local liver function than conventional CT images. Furthermore, Shuke *et al*^[9] reported that GSA was the best radioisotope for evaluating liver function by scintigraphy. Therefore, we merged SPECT images obtained using GSA (GSA-SPECT) with CT simulation images to prepare isodose curves. We then used the merged images for treatment planning for HCC, including cases with PVTT, hepatic vein tumor thrombus (HVTT) and/or bile tract tumor thrombus (BTTH)^[10,11]. We refer to this approach as SPECT-based three-dimensional conformal radiotherapy (SPECT-B-3DCRT).

The aim of this article is to describe the technical details, safety and efficacy of SPECT-B-3DCRT. We also describe its potential limitations and possible strategies to overcome its limitations.

COMBINING RT WITH TRANSCATHETER ARTERIAL CHEMOEMBOLIZATION

Transcatheter arterial chemoembolization (TACE) is perhaps the most widely performed multidisciplinary therapy for unresectable HCC^[12]. However, because

TACE is commonly ineffective in patients with HCC ≥ 5 cm in diameter or HCC with blood vessel invasion^[12,13], we combined SPECT-B-3DCRT together with TACE in such patients, with the aim of improving treatment outcomes^[10,11]. Namely, TACE was applied for intrahepatic metastasis out of the radiation field. RT is also applied to metastases in bone, liver and brain. Accordingly, TACE plus RT is an effective multidisciplinary therapy for patients with otherwise limited treatment options^[10,11,14-16].

DEFINITION OF FUNCTIONAL LIVER

There is increasing research into the use of GSA in internal medicine and surgery in the context of hepatology^[17,18], but it has been overlooked in relation to RT. When we first considered applying GSA-SPECT to RT, we found no reliable studies describing the potential relationship between GSA and RT. However, we found some studies describing the use of Tc-99m-macroaggregated albumin in RT of lung cancer. Although different radioisotopes are used for different cancers, these earlier reports highlighted the need to select an appropriate radioisotope and evaluate organ function before commencing RT^[19,20,21]. The first step for evaluating liver function involved fusing the SPECT image to the CT simulation image. The state of the liver varies considerably in HCC patients, ranging from normal liver function to Child C cirrhotic liver^[17]. Therefore, the next step was to establish a definition of functional liver. Unfortunately, a universal definition of functional liver cannot be used because the extent of cirrhotic liver varies considerably among patients. Christian *et al*^[19] proposed a threshold for organ function in individual organs. Based on a study by Sawamura *et al*^[22], we defined functional liver as the region of the liver in which radioisotope accumulation exceeded that of the HCC, while dysfunctional liver was defined as the region of the liver in which radioisotope accumulation was similar to that of the HCC^[10,11] (Figures 1 and 2). This definition of functional liver was therefore qualitative but not quantitative.

SPECT-B-3DCRT TECHNIQUE

The current Japanese guidelines for RT of HCC recommend that small HCCs are irradiated with 80-90 Gy in 40-45 fractions^[23]. However, surgical hepatectomy and radiofrequency ablation (RFA) are also used to treat small HCCs. At our institute, RT is generally requested for HCCs that cannot be managed surgically or by RFA, especially in patients with giant HCCs with intrahepatic metastasis and liver cirrhosis. All the patients in this series were asked by the surgeon and/or hepatologists to undergo radiotherapy because of the presence of PVTT. The administration of sorafenib was limited to liver function of Child-Pugh A classification and the cost of sorafenib, approximately 6000 dollars per month, was a financial burden on the patients. Surgical hepatic lobectomy was not scheduled because of the presence of

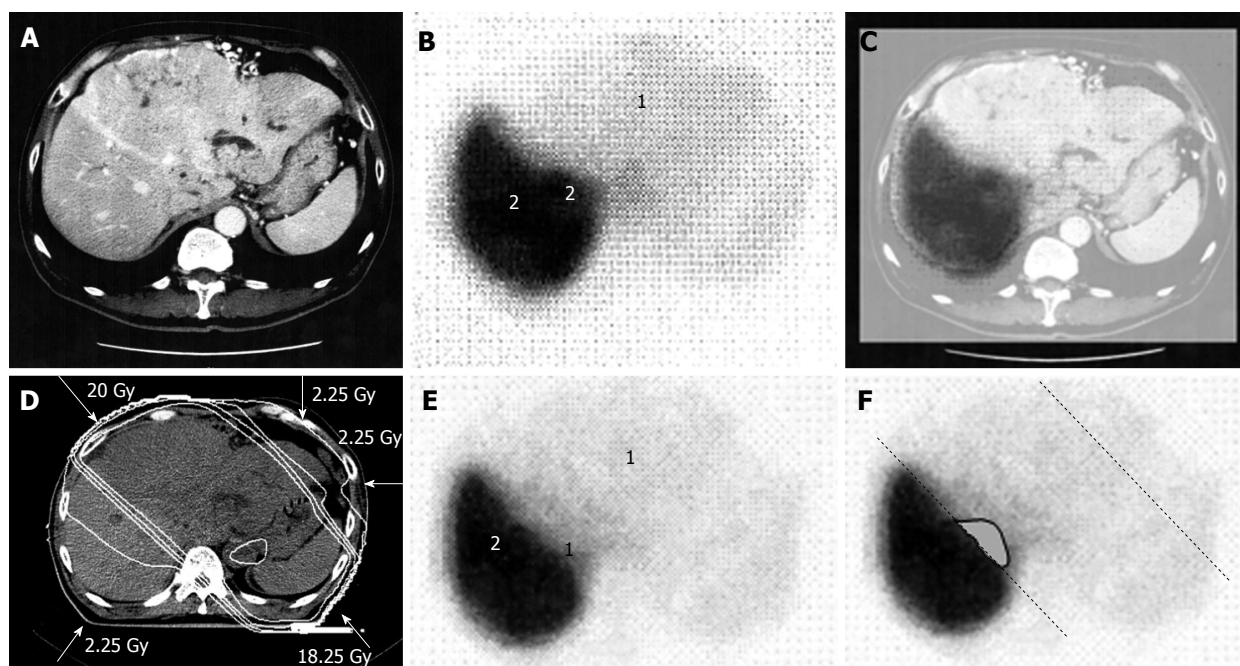


Figure 1 A 58-year-old man with hepatocellular carcinoma with a maximum diameter of 18.0 cm. A: Contrast-enhanced computed tomography; B: Single photon emission computed tomography with Tc-99m-galactosyl human serum albumin before radiotherapy; C: The merged image of A and B. The regions (1) without GSA accumulation in B correspond to main tumor located in the left lobe. The regions (2) of high accumulation in B correspond to functional liver. These regions were identified using the merged image (C); D: Dose distribution based on the CT simulation; E: GSA-SPECT image obtained 2 mo after RT shows regions without GSA accumulation (1) along the two high-dose beams, with preservation of functional liver (2); F: The extent of radiation-induced dysfunctional liver is shown as the gray area with a black border and was determined by comparing B and E. GSA: Galactosyl human serum albumin; SPECT: Single photon emission computed tomography; CT: Computed tomography; RT: Radiotherapy.

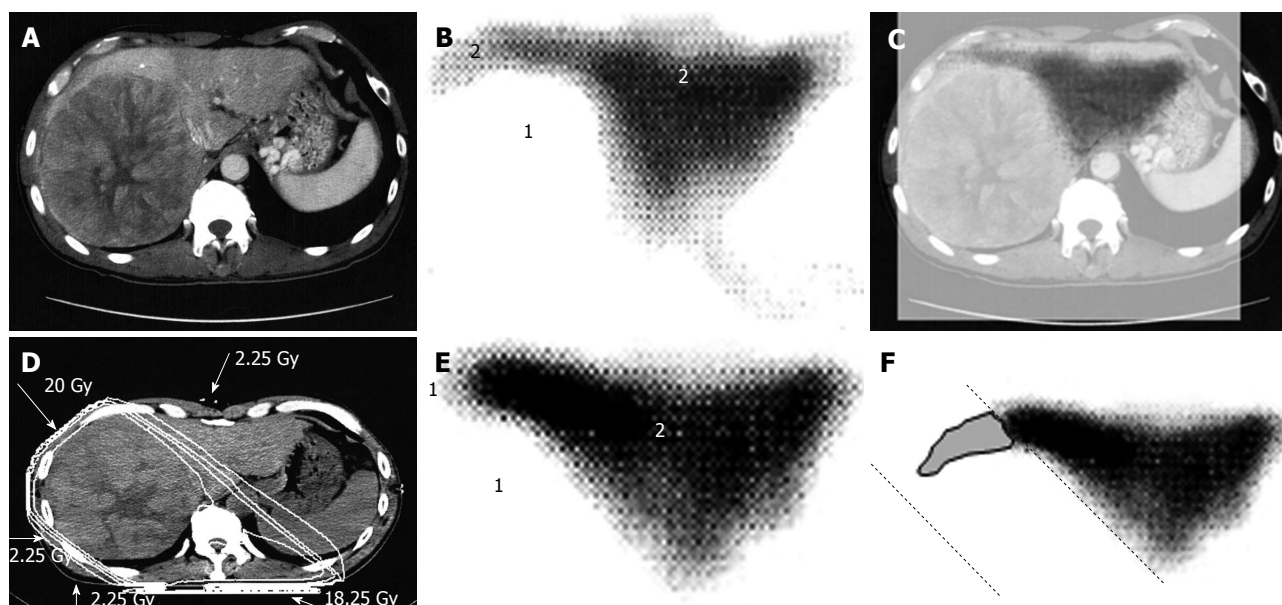


Figure 2 A 53-year-old man with hepatocellular carcinoma with a maximum diameter of 16.5 cm. A: Contrast-enhanced computed tomography; B: Single photon emission computed tomography with Tc-99m-galactosyl human serum albumin before radiotherapy; C: The merged image of A and B; The regions (1) without GSA accumulation in B correspond to main tumor located in the right lobe. The regions (2) of high accumulation in B correspond to functional liver. These regions were identified using the merged image (C); D: Dose distribution based on the CT simulation; E: GSA-SPECT image obtained 2 mo after RT shows regions without GSA accumulation (1) along the two high-dose beams, with preservation of functional liver (2); F: The extent of radiation-induced dysfunctional liver is shown as the gray area with a black border and was determined by comparing B and E. GSA: Galactosyl human serum albumin; SPECT: Single photon emission computed tomography; CT: Computed tomography; RT: Radiotherapy.

intrahepatic metastases in the other lobe. Namely, treatment of surgery and internal medicine were not indicated

for medical and social reasons. Therefore, we prescribed 45 Gy (18 fractions, 2.5 Gy/fraction) for the main tumor

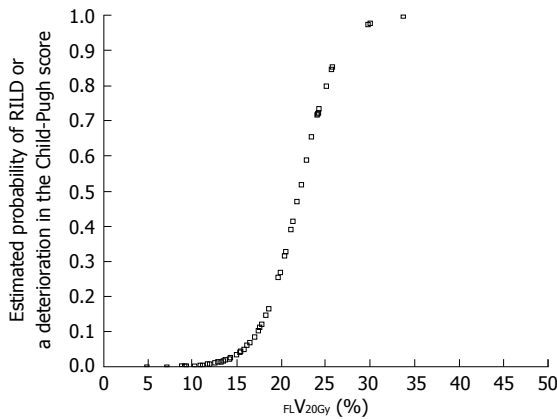


Figure 3 Estimated probability of radiation-induced liver disease or a deterioration in the Child-Pugh score by ≥ 1 point according to percentage of functional liver irradiated with ≥ 20 Gy (FLV_{20Gy}). Probability values were estimated by logistic regression analysis. RILD: Radiation-induced liver disease.

and the vessel tumor thrombus to prevent RILD^[11,15] (Figures 1 and 2). If the tumor size and/or type necessitated applying a greater dose to functional liver than was initially planned, we decided to omit some of the tumor from the irradiation field, providing that the omitted volume was $< 5\%$ of the whole tumor and was treated by TACE^[13]. Our objective was to avoid RILD in such cases. Furthermore, to account for respiratory mobilization^[2,3], the clinical target volume margin was routinely set 2-3 cm greater than the gross tumor volume margin. We also reduced the margin for respiration mobilization from 2-3 cm to 1 cm by asking the patients to hold their breath at the end of expiration^[10,11]. To minimize the effects of respiration, the patient practiced breath holding for 10-15 s at the end of expiration until the position could be maintained with a maximum variance of 5 mm under X-ray fluoroscopic monitoring. Treatment planning was also designed to reduce the radiation exposure to the liver^[10,11]. In short, the beam angle and dose preserved the functional volume visualized using the merged SPECT-CT image. We conducted SPECT-B-3DCRT in 64 patients with HCC, including 30 patients with Child B liver cirrhosis. We confirmed that a deterioration in the Child-Pugh score of 1 or 2 only occurred in patients when $> 20\%$ of the entire functional liver volume was irradiated with ≥ 20 Gy (Figures 3 and 4)^[16]. Figure 3 depicted the abrupt rise of FLV_{20Gy} from approximately 20% and Figure 4 depicted FLV_{20Gy} of 20% corresponded to the cutoff value in receiver operating characteristic analysis. Therefore, our treatment plan specified that $\leq 20\%$ of the functional liver volume would be irradiated with ≥ 20 Gy to minimize the deterioration in the Child-Pugh score.

The stomach, intestine, spinal cord and kidneys are at-risk organs during liver RT^[24,25]. The use of supplementary beams and/or setting a couch angle of $\leq 90^\circ$ helped to reduce irradiation of the stomach, intestine and spinal cord to ≤ 38.25 Gy, while $\leq 30\%$ of the total volume

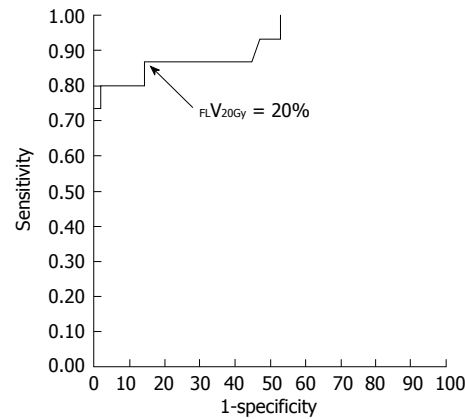


Figure 4 Receiver-operating characteristic curve for the percentage of functional liver volume irradiated with ≥ 20 Gy (FLV_{20Gy}). The optimal cutoff value for FLV_{20Gy} was 20% for predicting radiation-induced liver disease or a deterioration in the Child-Pugh score of ≥ 1 point. At this cutoff value, sensitivity and specificity were 0.867 and 0.857, respectively. The area under the receiver-operating characteristic curve was 0.923 ($P < 0.001$). *Journal of Gastroenterology and Hepatology Research* gave assurance that the copyright for this figure is retained by the authors.

of both kidneys was exposed to ≥ 20 Gy^[10,11].

The merged SPECT-CT images provided us with an unexpected but promising finding. The growth of gigantic HCCs is coupled with significant destruction of functional liver, especially of the tissue surrounding the tumor. Consequently, the target tissue becomes greater and it becomes easier to preserve functional liver with appropriate treatment planning^[14].

TREATMENT OF HCC ≥ 14 CM IN DIAMETER

Japanese RT guidelines suggest proton beam irradiation to treat HCC of ≥ 5 cm^[23]. Sugahara *et al.*^[26] reported that proton beam therapy brought about 2-year local tumor control rate of 87% and 2-year survival rate of 36%. These results seem to surpass our results below. However, median tumor size of their study was 11 cm (range, 10-14 cm) and proton beam therapy is not indicated for HCC of ≥ 14 cm^[26]. That is the reason why we introduced treating HCC of ≥ 14 cm using SPECT-B-3DCRT. We assessed the merged SPECT-CT images for HCC of ≥ 14 cm in diameter and found that the majority of functional liver was localized to the non-main HCC-bearing lobe rather than the main HCC-bearing lobe^[15] (Figures 1 and 2). Our clinical research indicated that SPECT-B-3DCRT did not affect liver function when $\geq 80\%$ of functional liver was located in the non-main HCC-bearing lobe^[15]. In 12 patients who received SPECT-B-3DCRT, the local tumor control rate was 78.6% and the 2-year survival rate was 33.3%, without serious adverse effects (Figure 5). Based on these findings, we recommend the use of SPECT-B-3DCRT for patients with gigantic (≥ 14 cm) HCC that cannot be managed by resection or proton beam therapy.

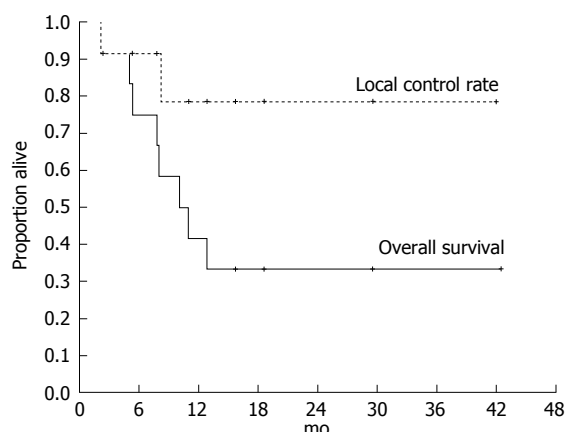


Figure 5 Kaplan-Meier analysis of the local control rate of the irradiated tumor and the survival in 12 cases of hepatocellular carcinoma exceeding 14 cm following single photon emission computed tomography-based three-dimensional radiotherapy. Cancer and Clinical oncology assurance that the copyright for this figure is retained by the authors.

TREATMENT OF HCC 5-14 CM IN DIAMETER

If functional liver is predominantly located in the non-main HCC-bearing lobe, SPECT-B-3DCRT can be performed without significant concerns, as described above. However, in some patients, the majority of functional liver is located in the main HCC-bearing lobe. If the main HCC-bearing lobe is the right lobe and $> 50\%$ of functional liver volume is in the main HCC-bearing lobe, the treatment strategy should be developed very carefully.

We treated 26 patients with HCCs of 5-14 cm with PVTT, leading to the control rate of 92.2% of the PVTT and 1-year and 2-year survival rate of 44.4% and 30%, respectively^[10]. Figure 6 shows a typical patient with an HCC of 5-14 cm in diameter. This patient had a right PVTT. SPECT revealed that 85% of functional liver was in the right lobe adjacent to the PVTT. If the RT plan was prepared for normal liver using CT images alone, we would expect that short-axis beams (hypothetical main beams, Figure 6F) would result in less irradiation of normal liver than that with long-axis beams (actual main beams, Figure 6C). $NL V_{20Gy}$ would be 30.8% for the long-axis beam plan and 23.1% for the short-axis beam plan. However, $FL V_{20Gy}$ based on SPECT images was 23.8% for the long-axis beam plan and 43.7% for the short-axis beam plan (Figure 7). Therefore, in this patient, RT using short-axis beams would likely cause RILD.

Cheng *et al.*^[2] reported that 17/89 (19.1%) and 7/89 (7.9%) patients who received 3DCRT with treatment planning without SPECT experienced RILD and fatal RILD, respectively. In the study by Liang *et al.*^[3], 17/109 (15.6%) and 13/109 (11.9%) patients developed RILD and fatal RILD, respectively. In our series, 3/64 (4.7%) and 0 patients (0%) who received SPECT-B-3DCRT experienced RILD and fatal RILD, respectively^[16]. Therefore, we believe that GSA-SPECT helps to predict and may ultimately reduce the risk of non-fatal and fatal RILD.

TREATMENT OF HCC < 5 CM IN DIAMETER

SPECT-B-3DCRT can be applied to HCC of ≤ 5 cm with PVTT, HVTT and/or BTTT. In this situation, functional liver surrounds the main tumor and is therefore likely to be damaged by RT. Regrettably, as we encountered no patient with HCC < 5 cm with PVTT^[10,11], we described the content of radiotherapy for HCC < 5 cm by referring to other manuscripts. Mornex *et al.*^[27] reported that 3DCRT caused Grade 4 toxicity in 2/11 (22%) Child B patients and Grade 3 toxicity in 3/16 (19%) Child A patients with a HCC ≤ 5 cm in diameter. Therefore, smaller HCCs require more careful treatment planning than larger HCCs. In this context, we consider that treatment planning with $FL V_{20Gy} \leq 20\%$ is an important approach for preserving functional liver (Figures 3 and 4). If $FL V_{20Gy}$ is $> 20\%$ of the planned volume of the main tumor to be irradiated, we suggest that the treatment plan is revised to omit part of the main tumor. This residual part of the tumor can be treated by TACE instead^[16].

LIMITATIONS OF FUNCTIONAL LIVER

If merged SPECT-CT images are available, the concept of functional liver is particularly useful for treatment planning in individual patients. However, functional liver is a qualitative rather than quantitative concept, making it difficult to compare data on functional liver among institutes. Therefore, an objective definition of functional liver should be established and standardized.

DOSE-FUNCTION HISTOGRAM AND FUNCTIONAL COUNT RATE (F_{Gy})

Sugahara *et al.*^[17] used GSA SPECT to evaluate the function of the right and left lobes before surgical hepatectomy in a quantitative manner by determining the liver uptake of GSA relative to the total dose of GSA injections. Christian *et al.*^[19] and Seppenwoolde *et al.*^[21] used lung perfusion SPECT for treatment planning and evaluated the extent of functional lung. Therefore, software has been developed to determine the dose-function histograms (DFH) from perfusion SPECT images for use in treatment planning for lung cancer^[20].

Based on these previous reports, we propose functional count rate (F_{Gy}) as a quantitative index of functional liver. F_{Gy} is defined as the percentage of the functional liver rate in the DFH and is based on V_{Gy} , the percentage of liver volume in the DVH. F_{Gy} is calculated using the following formula: $F_{Gy} = 100 \times (\text{GSA count in the area of the liver indicated by the isodose curve}) / (\text{GSA count for the entire liver})$. Because we use $FL V_{20Gy} \leq 20\%$ as a qualitative safety marker, F_{20Gy} was calculated for the patient presented in Figure 8. For this patient, F_{20Gy} , $NL V_{20Gy}$ and $FL V_{20Gy}$ were 22.2, 20.6 and 18.1, respectively. We consider that, because DFH and F_{Gy} link the area of the isodose curve to liver

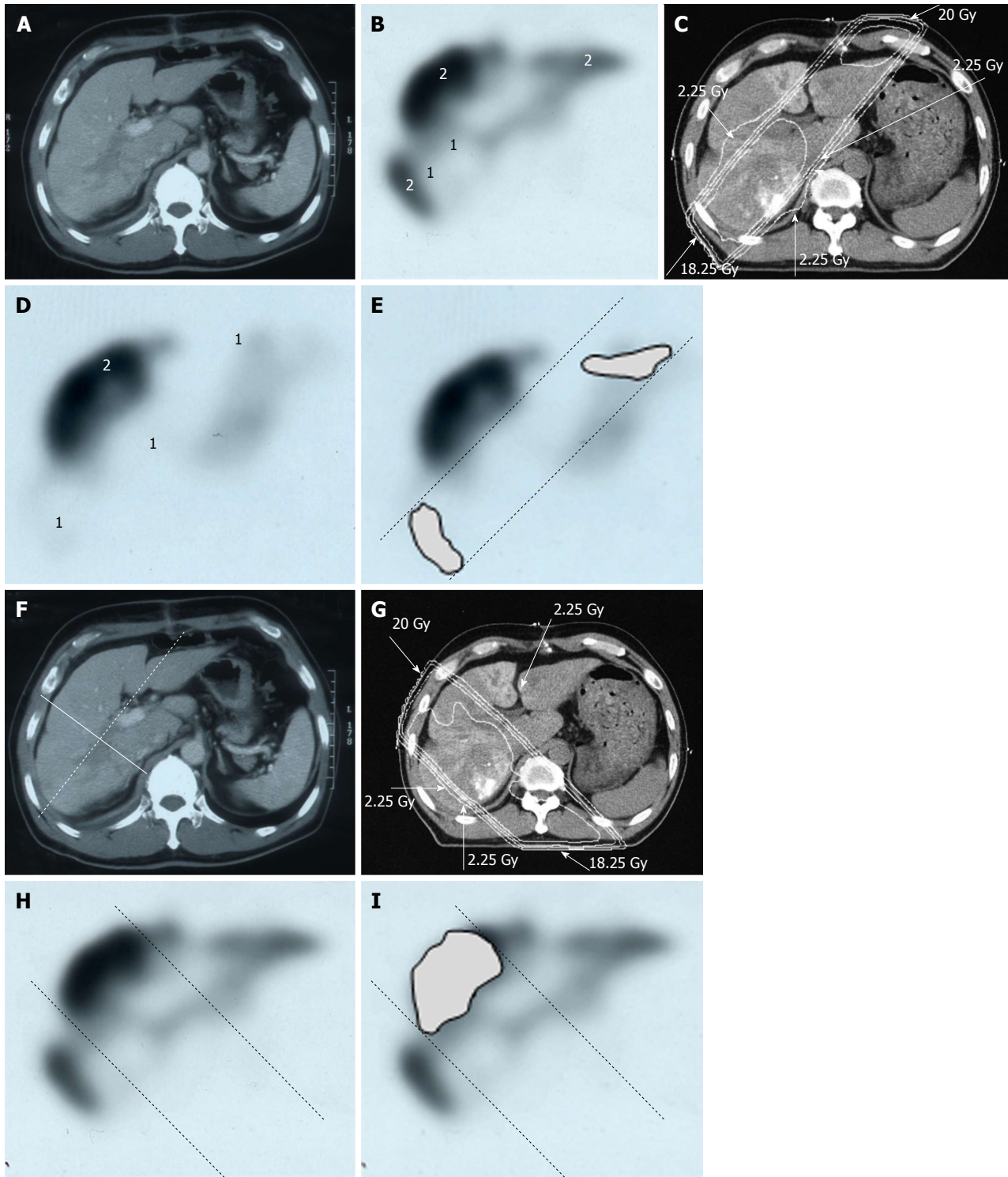


Figure 6 Distribution of functional liver and treatment planning for a 60-year-old male with hepatocellular carcinoma and liver cirrhosis of Child-Pugh grade A. A: Contrast-enhanced computed tomography shows a PVT in the right first portal vein originating from the right posterior sub-segment branch of the portal vein; B: GSA-SPECT taken before RT at the same level as A confirms that functional liver (2) is unevenly distributed between the anterior and lateral sides of the right PVT. 1 = dysfunctional liver; C: The two main radiation beams were angled in the left-anterior to right-posterior direction (20 Gy) and in the right-posterior to left-anterior direction (18.25 Gy beam); D: GSA-SPECT image obtained 2 mo after RT shows functional liver (2) and preservation of the right anterior sub-segment. This image also shows that the extent of dysfunctional liver has increased in the right posterior and left medial sub-segments; E: The extent of radiation-induced dysfunctional liver is shown as the dark gray area; F-I: Hypothetical treatment planning; F: The hypothetical main beams are angled in the right-anterior to left-posterior direction (solid lines), unlike the actual beams (dotted lines); G: The hypothetical radiation beams are angled in the right-anterior to left-posterior direction (20 Gy) and in the left-posterior to right-anterior direction (18.25 Gy). Although the radiation-induced destruction of normal liver can be estimated, it is difficult to predict the extent of radiation-induced destruction of functional liver from CT simulation alone; H: GSA-SPECT image together with the hypothetical main beams; I: The gray area indicates the extent of radiation-induced dysfunctional liver likely to be induced by the hypothetical main beams. The relative difference in the destruction of functional liver between the real and the hypothetical treatment plans can be estimated by comparing E and I. PVT: Portal vein tumor thrombus; GSA-SPECT: Galactosyl human serum albumin-single photon emission computed tomography with Tc-99m-galactosyl human serum albumin image; RT: Radiotherapy; CT: Computed tomography.

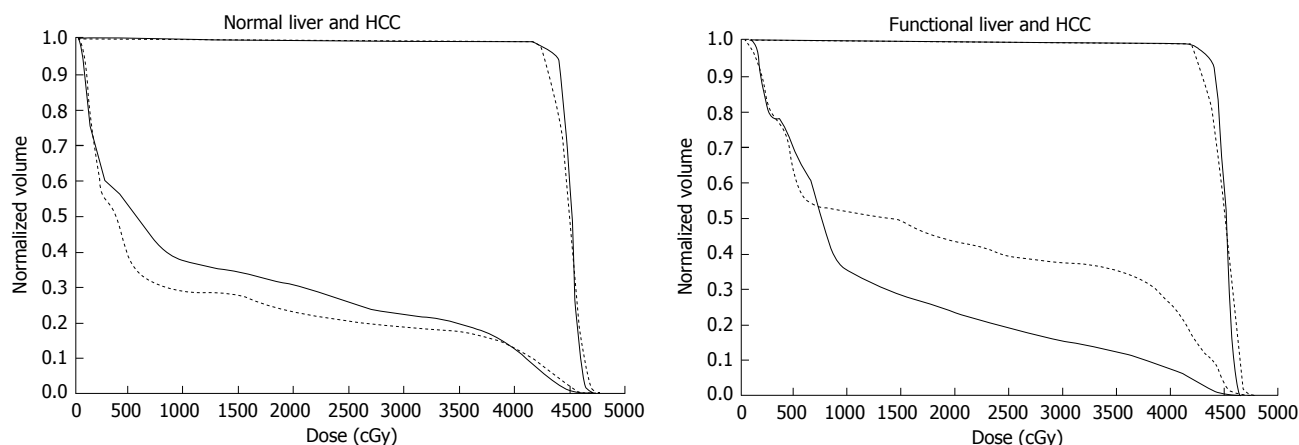


Figure 7 Comparison of dose-volume histograms between actual treatment plans (solid lines) and hypothetical treatment plans (dotted lines). A: Comparison of the DVH for normal liver. In this case, the percentage of the normal liver irradiated with ≥ 20 Gy (nLV_{20Gy}) was 23.1% for the hypothetical treatment plan vs 30.8% for the actual treatment plan. Therefore, irradiation of normal liver is lower for the hypothetical treatment plan than for the actual treatment plan; B: Comparison of the DVH for functional liver. In this case, the percentage of functional liver irradiated with ≥ 20 Gy (FLV_{20Gy}) was 43.7% for the hypothetical treatment plan vs 23.8% for the actual treatment plan. Therefore, irradiation of functional liver is lower for the actual treatment plan than for the hypothetical treatment plan. The difference between nLV_{20Gy} and FLV_{20Gy} in these two settings is due to the uneven distribution of functional liver. DVH: Dose-volume histograms; HCC: Hepatocellular carcinoma.

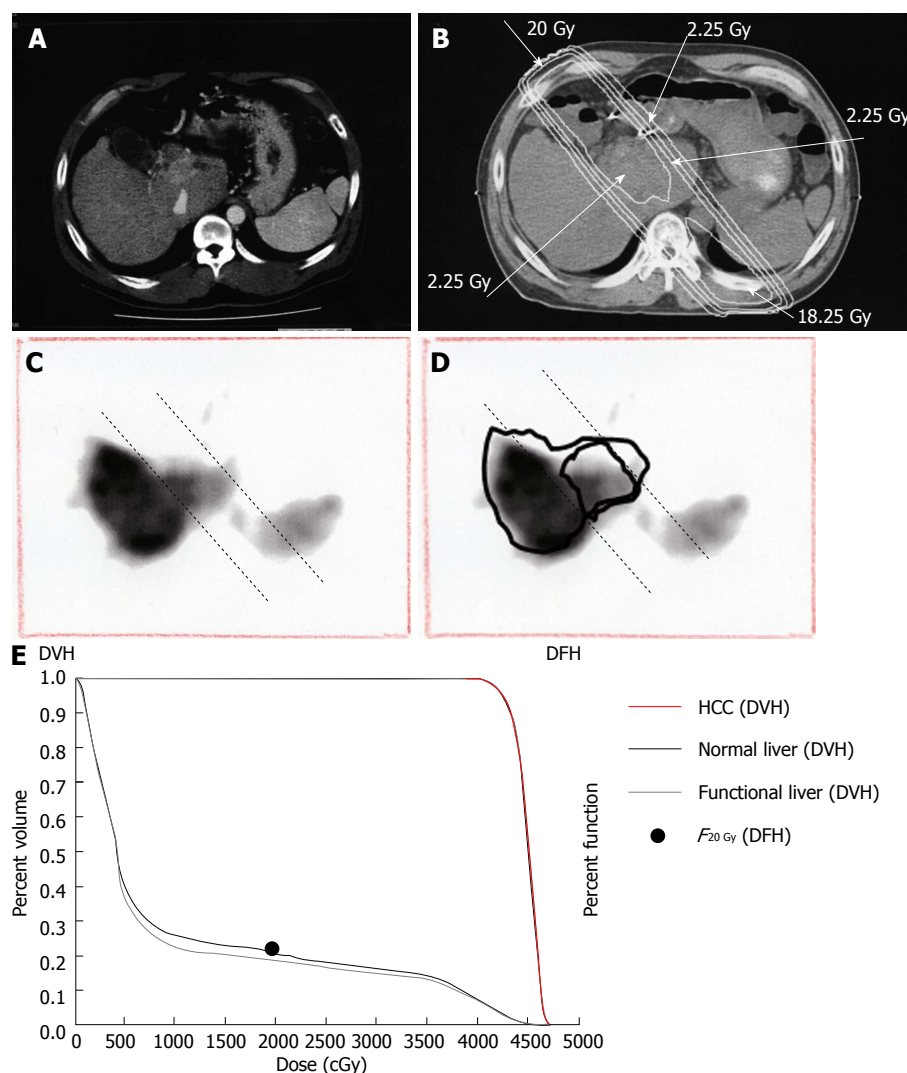


Figure 8 Quantitative analysis of radiation-induced dysfunctional liver. A: Computed tomographic image of a 52-year-old man with a recurrent tumor thrombus in the main portal vein after undergoing left hepatectomy for hepatocellular carcinoma; B: Isodose curves used for treatment planning; C: F_{20Gy} was calculated from the GSA count of the entire liver and the area within the 20 Gy isodose curve; D: F_{20Gy} was calculated from a single photon emission computed tomography with Tc-99m-galactosyl human serum albumin image using the formula: $F_{20Gy} = 100 \times (\text{GSA count in the area of the liver within the 20 Gy isodose curve}) / (\text{GSA count for the entire liver})$; E: In this patient, F_{20Gy} was 22.2%. GSA: Galactosyl human serum albumin; DVH: Dose volume histogram; DFH: Dose function histogram; HCC: Hepatocellular carcinoma.

function in a quantitative manner, they could replace DVH and V_{Gy} as gold-standard methods for evaluating the effects of RT on liver function. However, further studies are needed to confirm the clinical utility of DFH and F_{Gy} in treatment planning for patients with HCC and liver dysfunction.

CONCLUSION

SPECT-B-3DCRT combined with TACE can be performed in patients with HCC of any size, together with a PVTT, HVTT and/or BTIT, offering improved safety and therapeutic outcomes compared with existing modalities. Although $FLV_{20Gy} \leq 20\%$ is a qualitative assessment, it is a useful safety marker for predicting the risk of RILD. We also consider that DFH and F_{Gy} are promising quantitative markers for predicting the effects of SPECT-B-3DCRT in patients with HCC.

ACKNOWLEDGMENTS

Journal of Gastroenterology and Hepatology Research gave assurance that the copyright for this figure is retained by the authors.

REFERENCES

- Mohan R, Brewster LJ, Barest GD. A technique for computing dose volume histograms for structure combinations. *Med Phys* 1987; **14**: 1048-1052 [PMID: 3696069 DOI: 10.1118/1.595984]
- Cheng JC, Wu JK, Lee PC, Liu HS, Jian JJ, Lin YM, Sung JL, Jan GJ. Biologic susceptibility of hepatocellular carcinoma patients treated with radiotherapy to radiation-induced liver disease. *Int J Radiat Oncol Biol Phys* 2004; **60**: 1502-1509 [PMID: 15590181 DOI: 10.1016/j.ijrobp.2004.05.048]
- Liang SX, Zhu XD, Xu ZY, Zhu J, Zhao JD, Lu HJ, Yang YL, Chen L, Wang AY, Fu XL, Jiang GL. Radiation-induced liver disease in three-dimensional conformal radiation therapy for primary liver carcinoma: the risk factors and hepatic radiation tolerance. *Int J Radiat Oncol Biol Phys* 2006; **65**: 426-434 [PMID: 16690430 DOI: 10.1016/j.ijrobp.2005.12.031]
- Burman C, Kutcher GJ, Emami B, Goitein M. Fitting of normal tissue tolerance data to an analytic function. *Int J Radiat Oncol Biol Phys* 1991; **21**: 123-135 [PMID: 2032883 DOI: 10.1016/0360-3016(91)90172-Z]
- Lyman JT. Complication probability as assessed from dose-volume histograms. *Radiat Res Suppl* 1985; **8**: S13-S19 [PMID: 3867079 DOI: 10.2307/3583506]
- Kim TH, Kim DY, Park JW, Kim SH, Choi JL, Kim HB, Lee WJ, Park SJ, Hong EK, Kim CM. Dose-volumetric parameters predicting radiation-induced hepatic toxicity in unresectable hepatocellular carcinoma patients treated with three-dimensional conformal radiotherapy. *Int J Radiat Oncol Biol Phys* 2007; **67**: 225-231 [PMID: 17056199]
- Ikai I, Yamaoka Y, Yamamoto Y, Ozaki N, Sakai Y, Satoh S, Shinkura N, Yamamoto M. Surgical intervention for patients with stage IV-A hepatocellular carcinoma without lymph node metastasis: proposal as a standard therapy. *Ann Surg* 1998; **227**: 433-439 [PMID: 9527067]
- Nanashima A, Yamaguchi H, Shibasaki S, Morino S, Ide N, Takeshita H, Tsuji T, Sawai T, Nakagoe T, Nagayasu T, Oga-wa Y. Relationship between CT volumetry and functional liver volume using technetium-99m galactosyl serum albumin scintigraphy in patients undergoing preoperative portal vein embolization before major hepatectomy: a preliminary study. *Dig Dis Sci* 2006; **51**: 1190-1195 [PMID: 16944008 DOI: 10.1007/s10620-006-8031-x]
- Shuke N, Aburano T, Nakajima K, Yokoyama K, Sun BF, Matsuda H, Muramori A, Michigishi T, Tonami N, Hisada K. [The utility of quantitative ^{99m}Tc -GSA liver scintigraphy in the evaluation of hepatic functional reserve: comparison with ^{99m}Tc -PMT and ^{99m}Tc -Sn colloid]. *Kaku Igaku* 1992; **29**: 573-584 [PMID: 1434071]
- Shirai S, Sato M, Suwa K, Kishi K, Shimono C, Kawai N, Tanihata H, Minamiguchi H, Nakai M. Single photon emission computed tomography-based three-dimensional conformal radiotherapy for hepatocellular carcinoma with portal vein tumor thrombus. *Int J Radiat Oncol Biol Phys* 2009; **73**: 824-831 [PMID: 18755560 DOI: 10.1016/j.ijrobp.2008.04.055]
- Shirai S, Sato M, Suwa K, Kishi K, Shimono C, Sonomura T, Kawai N, Tanihata H, Minamiguchi H, Nakai M. Feasibility and efficacy of single photon emission computed tomography-based three-dimensional conformal radiotherapy for hepatocellular carcinoma 8 cm or more with portal vein tumor thrombus in combination with transcatheter arterial chemoembolization. *Int J Radiat Oncol Biol Phys* 2010; **76**: 1037-1044 [PMID: 19540053 DOI: 10.1016/j.ijrobp.2009.03.023]
- Yamada R, Sato M, Kawabata M, Nakatsuka H, Nakamura K, Takashima S. Hepatic artery embolization in 120 patients with unresectable hepatoma. *Radiology* 1983; **148**: 397-401 [PMID: 6306721]
- Arata S, Tanaka K, Okazaki H, Kondo M, Morimoto M, Saito S, Numata K, Nakamura S, Sekihara H. Risk factors for recurrence of large HCC in patients treated by combined TAE and PEI. *Hepatogastroenterology* 2001; **48**: 480-485 [PMID: 11379338]
- Shirai S, Sato M, Noda Y, Kishi K, Kawai N, Minamiguchi H, Nakai M, Sanda H, Sahara S, Ikoma A, Sonomura T. Distribution of functional liver volume in hepatocellular carcinoma patients with portal vein tumor thrombus in the 1st branch and main trunk using single photon emission computed tomography-application to radiation therapy. *Cancers (Basel)* 2011; **3**: 4114-4126 [DOI: 10.3390/cancers3044114]
- Shirai S, Sato M, Noda Y, Kishi K, Ikoma A, Sanda H, Sonomura T, Minamiguchi H, Nakai M, Kawai N. SPECT-based radiation therapy and transcatheter arterial chemoembolization for unresectable hepatocellular carcinoma sized 14 cm or greater. *Cancer Clin Oncol* 2012; **1**: 65-76 [DOI: 10.5539/cc.o.v1n1p65]
- Shirai S, Sato M, Noda Y, Kumayama Y, Sonomura T, Kawai N, Minamiguchi H, Nakai M, Sanda H, Tanaka F. The safety indicator of radiotherapy for advanced hepatoma with liver cirrhosis. *J Gastroenterol Hepatol Res* 2013; **2**: 730-736
- Sugahara K, Togashi H, Takahashi K, Onodera Y, Sanjo M, Misawa K, Suzuki A, Adachi T, Ito J, Okumoto K, Hattori E, Takeda T, Watanabe H, Saito K, Saito T, Sugai Y, Kawata S. Separate analysis of asialoglycoprotein receptors in the right and left hepatic lobes using Tc-GSA SPECT. *Hepatology* 2003; **38**: 1401-1409 [PMID: 14647051 DOI: 10.1053/jhep.2003.09031]
- Kaibori M, Ha-Kawa SK, Maehara M, Ishizaki M, Matsui K, Sawada S, Kwon AH. Usefulness of Tc- 99m -GSA scintigraphy for liver surgery. *Ann Nucl Med* 2011; **25**: 593-602 [PMID: 21800021 DOI: 10.1007/s12149-011-0520-0]
- Christian JA, Partridge M, Nioutsikou E, Cook G, McNair HA, Cronin B, Courbon F, Bedford JL, Brada M. The incorporation of SPECT functional lung imaging into inverse radiotherapy planning for non-small cell lung cancer. *Radiother Oncol* 2005; **77**: 271-277 [PMID: 16274762 DOI: 10.1016/j.radonc.2005.08.008]
- Marks LB, Sherouse GW, Munley MT, Bentel GC, Spencer DP. Incorporation of functional status into dose-volume analysis. *Med Phys* 1999; **26**: 196-199 [PMID: 10076973 DOI: 10.1118/1.598503]

- 21 **Seppenwoolde Y**, Muller SH, Theuws JC, Baas P, Belderbos JS, Boersma LJ, Lebesque JV. Radiation dose-effect relations and local recovery in perfusion for patients with non-small-cell lung cancer. *Int J Radiat Oncol Biol Phys* 2000; **47**: 681-690 [PMID: 10837952 DOI: 10.1016/S0360-3016(00)00454-5]
- 22 **Sawamura T**, Nakada H, Hazama H, Shiozaki Y, Sameshima Y, Tashiro Y. Hyperasialoglycoproteinemia in patients with chronic liver diseases and/or liver cell carcinoma. Asialoglycoprotein receptor in cirrhosis and liver cell carcinoma. *Gastroenterology* 1984; **87**: 1217-1221 [PMID: 6092193]
- 23 **Japanese Society for Therapeutic Radiology and Oncology.** Hepatocellular carcinoma. In: Radiotherapy planning guideline 2012 (in Japanese). Tokyo: Kinbara Pub, 2012: 161-164
- 24 **Emami B**, Lyman J, Brown A, Coia L, Goitein M, Munzenrider JE, Shank B, Solin LJ, Wesson M. Tolerance of normal tissue to therapeutic irradiation. *Int J Radiat Oncol Biol Phys* 1991; **21**: 109-122 [PMID: 2032882 DOI: 10.1016/0360-3016(91)90171-Y]
- 25 **Park W**, Lim DH, Paik SW, Koh KC, Choi MS, Park CK, Yoo BC, Lee JE, Kang MK, Park YJ, Nam HR, Ahn YC, Huh SJ. Local radiotherapy for patients with unresectable hepatocellular carcinoma. *Int J Radiat Oncol Biol Phys* 2005; **61**: 1143-1150 [PMID: 15752895 DOI: 10.1016/j.ijrobp.2004.08.028]
- 26 **Sugahara S**, Oshiro Y, Nakayama H, Fukuda K, Mizumoto M, Abei M, Shoda J, Matsuzaki Y, Thono E, Tokita M, Tsuboi K, Tokuyue K. Proton beam therapy for large hepatocellular carcinoma. *Int J Radiat Oncol Biol Phys* 2010; **76**: 460-466 [PMID: 19427743 DOI: 10.1016/j.ijrobp.2009.02.030]
- 27 **Mornex F**, Girard N, Beziat C, Kubas A, Khodri M, Trepo C, Merle P. Feasibility and efficacy of high-dose three-dimensional-conformal radiotherapy in cirrhotic patients with small-size hepatocellular carcinoma non-eligible for curative therapies--mature results of the French Phase II RTF-1 trial. *Int J Radiat Oncol Biol Phys* 2006; **66**: 1152-1158 [PMID: 17145534 DOI: 10.1016/j.ijrobp.2006.06.015]

P- Reviewer: Francica G, Kumar P, Picardi A **S- Editor:** Ji FF
L- Editor: Roemmele A **E- Editor:** Liu SQ





Published by **Baishideng Publishing Group Inc**

8226 Regency Drive, Pleasanton, CA 94588, USA

Telephone: +1-925-223-8242

Fax: +1-925-223-8243

E-mail: bpgoffice@wjgnet.com

Help Desk: <http://www.wjgnet.com/esps/helpdesk.aspx>

<http://www.wjgnet.com>

